Monthly Notices of the ROYAL ASTRONOMICAL SOCIETY

MNRAS **468,** 1236–1244 (2017)
Advance Access publication 2017 March 2

doi:10.1093/mnras/stx529

Scattering V-type asteroids during the giant planet instability: a step for Jupiter, a leap for basalt

P. I. O. Brasil,[1★] F. Roig,[1★] D. Nesvorný[2★] and V. Carruba[3]

[1] *Observatório Nacional, 20921-400 Rio de Janeiro, RJ, Brazil*
[2] *Southwest Research Institute, Boulder, CO 80302, USA*
[3] *Faculdade de Engenharia, Universidade Estadual Paulista, 12516-410 Guaratinguetá, SP, Brazil*

Accepted 2017 February 28. Received 2017 February 24; in original form 2016 July 26

ABSTRACT

V-type asteroids are a taxonomic class whose surface is associated with a basaltic composition. The only known source of V-type asteroids in the Main Asteroid Belt is (4) Vesta, which is located in the inner part of the Main Belt. However, many V-type asteroids cannot be dynamically linked to Vesta, in particular, those asteroids located in the middle and outer parts of the Main Belt. Previous works have failed to find mechanisms to transport V-type asteroids from the inner to the middle and outer belts. In this work, we propose a dynamical mechanism that could have acted on primordial asteroid families. We consider a model of the giant planet migration known as the jumping Jupiter model with five planets. Our study is focused on the period of 10 Myr that encompasses the instability phase of the giant planets. We show that, for different hypothetical Vesta-like paleo-families in the inner belt, the perturbations caused by the ice giant that is scattered into the asteroid belt before being ejected from the Solar system are able to scatter V-type asteroids to the middle and outer belts. Based on the orbital distribution of V-type candidates identified from the Sloan Digital Sky Survey and the VISTA Survey colours, we show that this mechanism is efficient enough provided that the hypothetical paleo-family originated from a 100 to 500 km crater excavated on the surface of (4) Vesta. This mechanism is able to explain the currently observed V-type asteroids in the middle and outer belts, with the exception of (1459) Magnya.

Key words: minor planets, asteroids: general – planets and satellites: dynamical evolution and stability.

1 INTRODUCTION

V-type asteroids are a particular taxonomic class of asteroids (e.g. Bus & Binzel 2002; DeMeo et al. 2009) whose surface mineralogy is associated with a basaltic composition (Burbine et al. 2001). Many V-type asteroids in the Main Belt, the so-called vestoids, belong to a collisional family, the Vesta family (Binzel & Xu 1993; Milani et al. 2014), located in the inner belt ($2.1 < a < 2.5$ au). This family originated by one or more cratering events that excavated the basaltic surface of asteroid (4) Vesta between 1 and 3 Gyr ago (Russell et al. 2012; Schenk et al. 2012; Buratti et al. 2013). Many other V-type asteroids, which we will refer to as the non-vestoids, do not belong to the current Vesta family and cannot be directly related to any specific collisional event. In particular, this is the case of those V-type asteroids located in the middle ($2.5 < a < 2.8$ au) and the outer ($2.8 < a < 3.2$ au) Main Belt, like (1459) Magnya (e.g. Lazzaro et al. 2000; Roig & Gil-Hutton 2006; Moskovitz et al. 2008; de Sanctis et al. 2011a). Neither large basaltic parent bodies like (4) Vesta nor V-type asteroid families are known in these regions. In this work, we investigate the possibility that some non-vestoid V-type asteroids have been scattered from the inner belt during the instability period related to the radial migration of the outer planets, some 4 Gyr ago (Tsiganis et al. 2005; Morbidelli et al. 2009; Nesvorný & Morbidelli 2012).

Our focus is on the effect of the 'jumping Jupiter' instability of the giant planets (Morbidelli et al. 2009) over the dynamics of V-type asteroids originated in the inner belt. This instability occurs while the giant planets are migrating by interaction with a disc of planetesimals exterior to Neptune's orbit during the so-called planetesimal-driven migration (Fernandez & Ip 1984; Tsiganis et al. 2005). The instability is related to a phase of mutual close encounters between the planets, which eventually leads to the ejection of a Neptune-sized ice giant after a scattering by Jupiter (Nesvorný 2011; Nesvorný & Morbidelli 2012). In this context, the model requires the initial existence of at least five planets: Jupiter, Saturn and three ice giants. The encounters make Jupiter and the other giants to undergo

★ E-mail: pedro_brasil87@hotmail.com (PIOB); froig@on.br (FR); davidn@boulder.swri.edu (DN)

© 2017 The Authors
Published by Oxford University Press on behalf of the Royal Astronomical Society

Downloaded from https://academic.oup.com/mnras/article-abstract/468/1/1236/3059980 by Universidade Estadual Paulista Jï¿½lio de Mesquita Filho user on 19 June 2019

rapid and large variations of their orbits. In particular, Jupiter's eccentricity is excited to its present value, and its semimajor axis 'jumps' inwards by ∼0.3–0.5 au. Also, the period ratio between Jupiter and Saturn changes from an initial ratio of 1.5 to the current ∼2.5 in a few tens of thousands of years. This behaviour satisfies the terrestrial planet constraint in that Jupiter's orbit discontinuously evolves during planetary encounters (Brasser et al. 2009), thus avoiding secular resonances that would otherwise lead to the disruption of the terrestrial planet system. The model also satisfies several other constraints imposed by the different populations of minor bodies (Nesvorný, Vokrouhlický & Morbidelli 2013; Brasil, Nesvorný & Gomes 2014; Deienno et al. 2014; Nesvorný et al. 2014a; Nesvorný, Vokrouhlický & Deienno 2014b; Nesvorný 2015a; Roig & Nesvorný 2015).

Brasil et al. (2016) have shown that the jumping Jupiter instability with five giant planets can disperse the asteroid collisional families that formed before or during the instability beyond recognition, which would help to explain the current paucity of asteroid families older than ∼3 Gyr (Carruba et al. 2016). A key ingredient in this phenomenon is the scattering of asteroids caused by the interactions with the fifth planet that is ejected from the system. This ice giant can reach heliocentric distances as small as 1.5–2.0 au before being ejected, thus sweeping the asteroid belt during a short period of time. Roig & Nesvorný (2015) have shown that, in some cases, this scattering can lead the asteroids to undergo semimajor axis changes of up to 0.5–1.0 au. Therefore, the jumping Jupiter instability provides a possible mechanism to implant V-type asteroids from the inner belt into the middle and outer belts.

This paper is organized as follows. In Section 2, we discuss the distribution of V-type and basaltic asteroids in the Main Belt and the previous efforts to assess their dynamics and to understand their origin. Section 3 describes the methodology applied to this study. Our results are presented in Section 4. The last section is devoted to conclusions.

2 BASALTIC ASTEROIDS IN THE MAIN BELT

Basalt is expected to originate during the process of geochemical differentiation in the interior of the largest asteroids. The paradigm of this model is asteroid (4) Vesta (Russell et al. 2012), a body of ∼500 km in diameter D, which has been identified long ago to own a basaltic crust (McCord, Adams & Johnson 1970; Zuber et al. 2011). The differentiation process was probably more efficient in the inner part of the Main Belt, where the temperature gradient favours the condensation of refractory and volatile-poor elements, in particular, the radioisotope ^{26}Al whose decay is mainly responsible for the heating in the asteroids interiors (Grimm & McSween 1993). This idea is supported by the fact that (4) Vesta itself is in the inner belt and also by the fact that the fraction of volatile-rich over volatile-poor asteroids with $D > 50$ km is three to eight times larger in the middle/outer belt than in the inner belt (e.g. Michtchenko, Lazzaro & Carvano 2016). The second largest known V-type asteroid is (1459) Magnya, a $D \sim 17$ km body located in the outer belt (Lazzaro et al. 2000; Delbo et al. 2006), and the remaining known V-type asteroids, both vestoids and non-vestoids, are all smaller than 7 km in diameter. In principle, it would not be expected to occur differentiation in such small bodies, and similarly to the vestoids and the Vesta family, the origin of non-vestoid V-types should be most likely related to the collisional fragmentation of large differentiated parent bodies (e.g. Michtchenko et al. 2002; Carruba, Michtchenko & Lazzaro 2007b).

2.1 Dynamics

So far, the only confirmed source of basaltic material in the Main Belt is (4) Vesta. Therefore, several works have been devoted to try to establish a dynamical link between (4) Vesta and the non-vestoid V-type asteroids. The interplay between mean motion resonances, secular resonances and the Yarkovsky effect (Bottke et al. 2002) has been addressed by Carruba et al. (2005) and Nesvorný et al. (2008), who found that many non-vestoids in the inner belt can originate as fugitives from the Vesta family over Gyr time-scales. These mechanisms, however, are not enough to explain a set of V-type asteroids in the inner belt showing lower orbital inclinations, on average, than the current Vesta family. Carruba et al. (2007a) studied the effect of close encounters between small vestoids and (4) Vesta, and concluded that the role of this mechanism in generating non-vestoids is minor. Roig et al. (2008) and Folonier, Roig & Beaugé (2014) analysed the crossing probability of small vestoids through the 3:1 mean motion resonance with Jupiter, driven by the Yarkovsky effect. They found that this mechanism would not be enough to explain the presence of several km-sized V-type asteroids in the middle belt. Finally, Ribeiro & Roig (2011) considered the transport of V-type asteroids from the inner belt through a Mars crossing regime combined with resonance stickiness and concluded that this mechanism is not able to implant V-type asteroids beyond 2.5 au in long-term stable orbits. In summary, long-term dynamics proved to be insufficient to link a significant fraction of the non-vestoid V-types to (4) Vesta.

Following these results, we will refer hereafter to four dynamical populations amongst the V-type asteroids.

(i) The vestoids, which correspond to the Vesta family members.

(ii) The fugitives population, i.e. the non-vestoids in the inner belt that can be dynamically related to (4) Vesta and/or to the Vesta family; these correspond to objects with $a \lesssim 2.3$ au or $I \gtrsim 6^\circ$.

(iii) The low-inclination inner belt population, i.e. the non-vestoids in the inner belt that shows no dynamical link to (4) Vesta at all; these correspond to objects with $a \gtrsim 2.3$ au and $I \lesssim 6^\circ$.

(iv) The middle/outer belt population of non-vestoids, which correspond to objects with $a > 2.5$ au.

Fig. 1 summarizes the orbital distribution of the 138 currently known V-type asteroids in the Main Belt confirmed from spectroscopic observations and identifies the different populations defined above. This figure compiles data from Duffard & Roig (2009), de Sanctis et al. (2011a,b), Ieva et al. (2016) and Migliorini et al. (2017).

In the above context, (1459) Magnya and the other middle/outer belt V-types, in particular, result to be the most paradoxical cases. The possibility of a local origin of (1459) Magnya was first addressed by Michtchenko et al. (2002), who proposed that, if this asteroid formed from the collisional breakup of a larger differentiated parent body in the outer belt, the subsequent family of Magnya would be dispersed beyond recognition over hundreds of Myr time-scales. However, even if such a hypothetical family would not be recognized nowadays as a dynamical family (i.e. a cluster of asteroid sharing similar orbital properties), footprints of its existence should be present in the outer belt. In particular, we should expect to find other V-type asteroids there besides (1459) Magnya.[1] As we can see in Fig. 1, the shortage of V-type asteroids beyond

[1] In a different context, Carruba et al. (2016) found that asteroid paleo-families (i.e. families formed about or more than 4 Gyr ago) would be able to dynamically disperse beyond recognition over the age of the Solar system, but footprints of them should be still detectable in the Main Belt.

Downloaded from https://academic.oup.com/mnras/article-abstract/468/1/1236/3059980 by Universidade Estadual Paulista Jï¿½lio de Mesquita Filho user on 19 June 2019

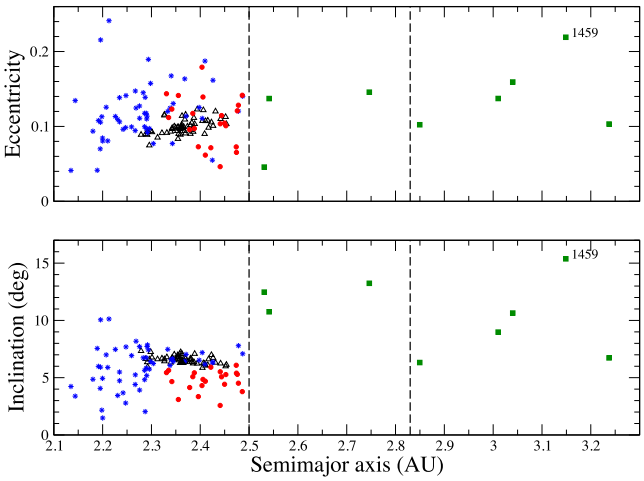

Figure 1. The orbital distribution of the 138 spectroscopic V-type asteroids in the Main Belt, compiled by different authors (see the text). The black full triangle represents (4) Vesta. The different populations are represented by black open triangles (vestoids), blue stars (fugitives), red full circles (low-inclination inner belt) and green full squares (middle/outer belt), respectively. (1459) Magnya is indicated by its number. The vertical dashed lines indicate the approximate boundaries of the inner, middle and outer asteroid belts.

2.5 au contrasts with the overabundance observed in the inner belt, where the Vesta family formed. This shortage may partly be due to observational bias, but a similar trend is observed when considering candidate V-type asteroids selected from the visible colours of the Sloan Digital Sky Survey (SDSS; Roig & Gil-Hutton 2006; Moskovitz et al. 2008; Carvano et al. 2010; Carruba et al. 2014; Huaman, Carruba & Domingos 2014) as well as from the infrared colours of the VISTA Survey (MOVIS; Licandro et al. 2017). Actually, the fraction of V-type asteroids in the middle/outer belt with respect to the total number of V-type asteroids are of only ∼4–6 per cent not only in the spectroscopic sample shown in Fig. 1 but also in the SDSS (e.g. Carvano et al. 2010) and the MOVIS samples. This, together with the fact that volatile-poor materials would not have been abundant in the outer asteroid belt, seems to point against the idea of a local origin of (1459) Magnya.

Concerning the other V-type asteroids in the middle/outer belt, Carruba et al. (2007b) first proposed that some middle belt V-types could be fragments of a collisional disrupted differentiated parent body whose best candidate would be asteroid (15) Eunomia (Nathues et al. 2005), located at 2.64 au. Eunomia has associated a collisional family, and the three spectroscopic V-types presently known in the middle belt could be interpreted as dynamical fugitives from this family. On the other hand, no spectroscopic V-types are known within the Eunomia family; only some SDSS V-type candidates were actually reported as family members (Carruba et al. 2014), but none of these candidates have been observed spectroscopically so far. Carruba et al. (2014) and Huaman et al. (2014) analysed the dynamics of the SDSS photometric V-types in the middle/outer belt and concluded that they are segregated into eight regions in the *a*–*I* plane which are dynamically isolated from each other. This led the authors to propose that at least eight different sources of basaltic material, either local or from Vesta, would be necessary to explain the current sample of candidate V-types beyond 2.5 au.

2.2 Surface properties

Observational evidence indicates that some V-type asteroids in the Main Belt show mineralogical properties that are incompatible with those of (4) Vesta (e.g. Hardersen, Gaffey & Abell 2004; Duffard et al. 2006; Duffard & Roig 2009), suggesting an origin from other (unknown) basaltic parent bodies. Recently, Ieva et al. (2016) gathered the available spectroscopic observations of several known V-type asteroids and analysed them using a uniform procedure to determine their mineralogical properties. They found that (1459) Magnya and the other non-vestoids located beyond 2.5 au have somehow distinctive spectroscopic properties from those of the vestoids and non-vestoids in the inner belt, supporting the idea that (1459) Magnya and the other middle/outer belt V-type asteroids are not genetically related to (4) Vesta.

Gil-Hutton, López-Sisterna & Calandra (2017) reported polarimetric measurements of 28 Main Belt V-type asteroids and found that they can be classified into two groups: (i) those that show measurements compatible with the polarimetric curve of (4) Vesta and (ii) those that show measurements compatible with the polarimetric curve of (1459) Magnya.[2] The first group includes several vestoids and inner belt non-vestoids, while the second group includes some inner belt vestoids and non-vestoids, as well as middle/outer belt non-vestoids.

It is worth noting that the errors involved in the determination of spectroscopic and polarimetric parameters are usually large. In many cases, the differences observed amongst the samples fall within their 1σ uncertainties, making them indistinguishable in practice. In principle, there is no clear relation between these spectroscopic and polarimetric differences and the different dynamical populations.

2.3 Size distribution

So far, the clearest evidence that prevents a link between (4) Vesta and (1459) Magnya is the size of the latter, which does not fit within the expected size frequency distribution (SFD) of the ejecta from craterization events (Durda et al. 2007; Michel et al. 2015) like those that excavated the surface of (4) Vesta. On the other hand, the remaining non-vestoids (from both the spectroscopic and SDSS samples) are all as small as the vestoids and may also have originated from craterization events. Images of Vesta's surface taken by the Dawn probe revealed two large basins in the south pole of the asteroid. One of them, named Rheasilvia with ∼500 km of diameter, has been dated ∼1 Gyr ago. The other one, named Veneneia with ∼400 km of diameter, has been dated 2–3 Gyr ago (Marchi et al. 2012). While Rheasilvia is the likely source of the current vestoids (Buratti et al. 2013; McSween et al. 2013), Veneneia could be the source of several non-vestoids (Schenk et al. 2012). Pirani & Turrini (2016) studied the formation of large basins on the surface of (4) Vesta during the epoch of the giant planet instability and concluded that any record of such basins would have been erased by the subsequent crater saturation over the age of the Solar system. This is in line with the fact that observed craters on Vesta's surface dated less than ∼4.1 Gyr ago (O'Brien et al. 2014). Therefore,

[2] Cellino et al. (2016) have shown that the polarimetric curve of (4) Vesta presents variations related to different albedo, composition and/or rugosity over its surface. Nevertheless, these variations are not enough to account for the differences with respect to the polarimetric curve of (1459) Magnya. In particular, the inversion angle of Vesta is ∼2° greater than that of Magnya, and this parameter is not sensitive to the changes on Vesta's surface.

Downloaded from https://academic.oup.com/mnras/article-abstract/468/1/1236/3059980 by Universidade Estadual Paulista Jï¿½lio de Mesquita Filho user on 19 June 2019

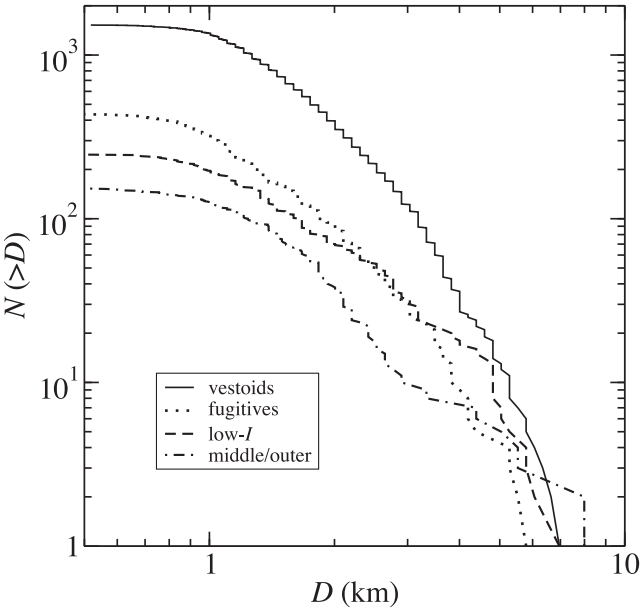

Figure 2. The cumulative size frequency distribution of the photometric V-type candidates in the Main Belt observed by the SDSS. Diameters are estimated assuming an albedo of 0.4. The different populations refer to those shown in Fig. 1.

the possibility of a very early craterization event on the surface of (4) Vesta that led to the origin of a Vesta-like family cannot be ruled out.

In this context, it is interesting to discuss the SFD of the different dynamical populations of V-type asteroids. This is shown in Fig. 2 for the sample of SDSS V-type candidates, but a similar result was obtained by Nesvorný et al. (2008) considering the spectroscopic sample. The fugitives population shows a similar SFD to the vestoids, indicating that these two populations may be related and have the same collisional age. On the other hand, the low-inclination population and the middle/outer population show SFDs that differ from the Vesta family, suggesting that these populations have a different origin/age. These populations (excluding (1459) Magnya due to its size) could have been originated by early craterization events on the surface of (4) Vesta, like the Veneneia basin or even older events (Schenk et al. 2012; McSween et al. 2013).

3 METHODS

Our goal in this study is to determine whether or not the jumping Jupiter instability could explain the orbital distribution of the non-vestoids, in particular, those in the middle/outer belt, assuming that they formed on a very early craterization event on (4) Vesta's surface. We have proceeded in the same way as described by Brasil et al. (2016). In short, we have generated Vesta-like synthetic families, i.e. artificial families with orbital parameters similar to those of (4) Vesta, using an algorithm that produces an initial orbital distribution of N family members assuming that their ejection velocities $v_{\rm ej}$ from the parent body follow a Maxwell distribution, with given mean $\bar{v}_{\rm ej}$. The smaller the mean ejection velocity, the more compact the initial family. Orbital elements of each member are then obtained from the ejection velocities using Gauss formulas, for the given values of the orbital elements of the parent body: semimajor axis a, eccentricity e, inclination I, true anomaly f and argument of perihelion ω. In all cases, we have considered $a = 2.36$ au. We have also considered $f = 90^\circ$ and $f + \omega = 0^\circ$, which produces rather spherical distributions in the space of orbital elements. The other parameters have been chosen in order to produce four different orbital set-ups: (i) a low-e and low-I initial family ($e = 0.089$, $I = 7\overset{\circ}{.}14$); (ii) a low-$e$ and high-I family ($e = 0.089$, $I = 15^\circ$); (iii) a high-e and low-I family ($e = 0.2$, $I = 7\overset{\circ}{.}14$) and (iv) a high-$e$ and high-I family ($e = 0.2$, $I = 15^\circ$). In addition, for each of these four set-ups, we considered two different values of $\bar{v}_{\rm ej}$: 100 and 500 m s^{-1}, representing a very compact and a very dispersed initial family, respectively. The initial number of members, N, was set to 1000 for the compact families and 5000 for the dispersed ones. This makes a total of eight different initial configurations.

The family members have been considered as massless test particles, subject to the gravitational perturbation of the giant planets only. To simulate the evolution of the giant planets during the jumping Jupiter instability, we have used a hybrid version of the SWIFT_RMVS3 symplectic integrator (Roig & Nesvorný 2015) that reads the positions and velocities of the planets from a file where they were previously stored at 1 yr intervals and interpolates them to the desired time-step using a two-body approach (Nesvorný 2011). The jumping Jupiter evolutions have been previously developed by Nesvorný & Morbidelli (2012). We have considered here 10 of these evolutions, including the ones identified as *case_1* and *case_3* in Brasil et al. (2016). The simulations lasted for 10 Myr. We recall that terrestrial planets have not been included in these simulations.

4 RESULTS

As expected from our previous study, the jumping Jupiter instability disperses the hypothetical families through two different mechanisms: (i) scattering of the asteroids due to close encounters with the fifth giant planet before its ejection and (ii) interaction of the asteroids with sweeping secular and mean motion resonances with the planets. The first mechanism is responsible for the dispersion in the semimajor axis, while the second causes the dispersion in eccentricity and inclination. We found that all the jumping Jupiter evolutions considered here were able to scatter Vesta-like family members beyond 2.5 au. The scattering efficiency depends on two factors. The first, and most important one, is the specific evolution of the fifth giant. In some evolutions, this planet reaches heliocentric distances as small as 1.5 au, thus strongly sweeping and scattering the inner part of the Main Belt. In other evolutions, the fifth planet does not reach the inner belt and the scattering effect is minimum. The second factor that influences the scattering efficiency is the particular initial configuration of the family.

Fig. 3 shows the typical results for a given jumping Jupiter evolution causing moderate scattering (*case_1*) and the four initially compact families. These figures resemble the situation observed in Fig. 1, i.e. a concentration of asteroids in the inner belt, and a few isolated bodies in the middle/outer belt. The gap that is observed in the inner belt around $I \sim 15^\circ$–20° is related to the ν_6 secular resonance. In principle, the group of orbits with $I > 20^\circ$ is mostly in the region of terrestrial planet crossing orbits and should be later eliminated by close encounters in a few 10^7 yr if the terrestrial planets were included in the simulations. As we will see later, the terrestrial planets will also be responsible for the long-term depletion of most of the orbits that remain in the inner belt after the instability.

Our results should be analysed from a probabilistic point of view, and we should not expect to precisely reproduce the current distribution of the non-vestoid V-type asteroids. Nevertheless, we have verified that, in general, the final inclinations of the dispersed family

Downloaded from https://academic.oup.com/mnras/article-abstract/468/1/1236/3059980 by Universidade Estadual Paulista Jï¿½lio de Mesquita Filho user on 19 June 2019

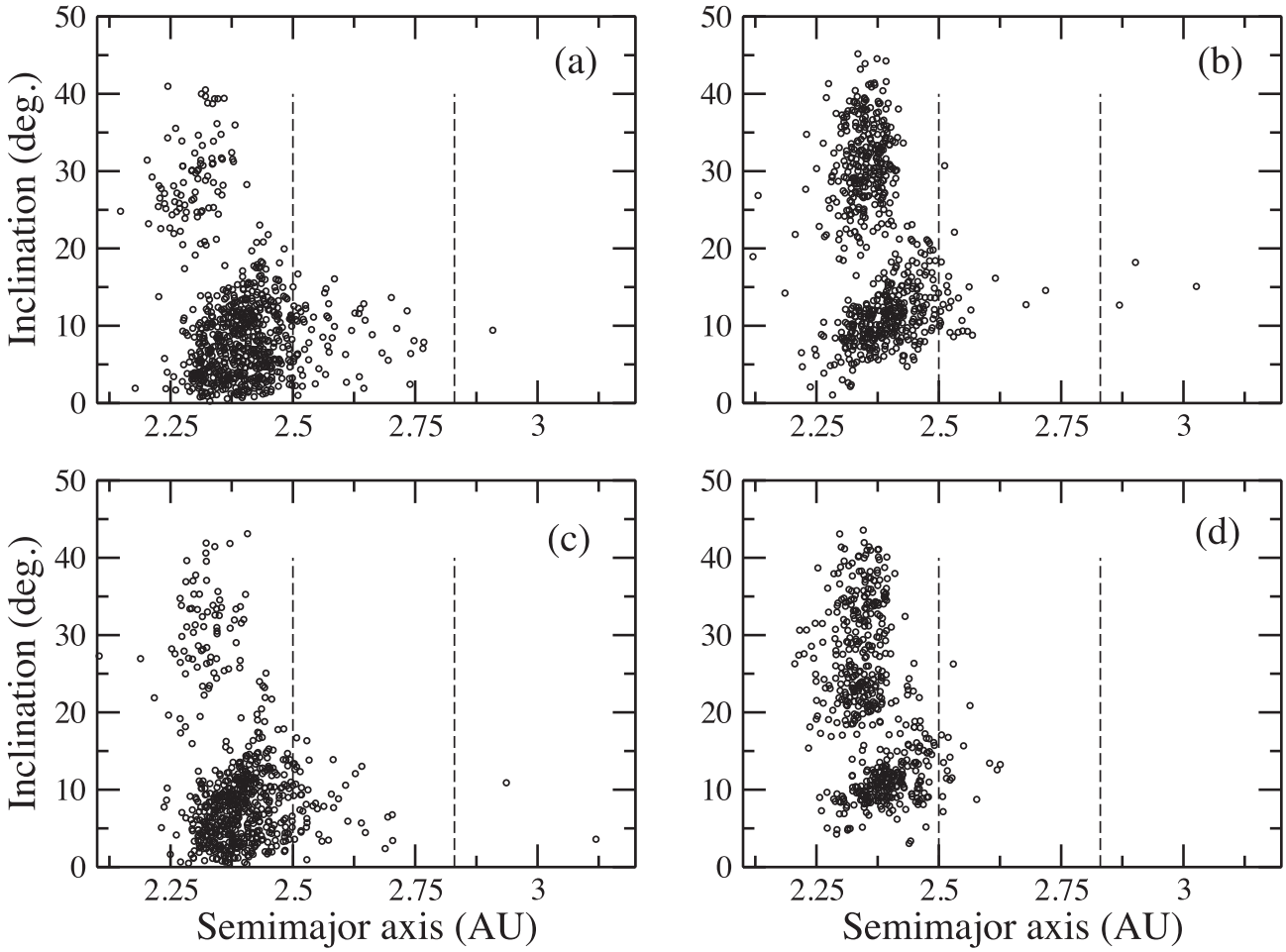

Figure 3. The final orbital distribution of four hypothetical Vesta-like families in the inner asteroid belt, after evolving through a jumping Jupiter instability (*case_1*). All the families are initially very compact, consistent with a mean ejection velocity of 100 m s^{-1}. The different panels correspond to the different orbital parameters of the parent body: (a) $e = 0.089$, $I = 7\overset{\circ}{.}14$; (b) $e = 0.089$, $I = 15^\circ$; (c) $e = 0.2$, $I = 7\overset{\circ}{.}14$ and (d) $e = 0.2$, $I = 15^\circ$. In all cases, the parent body had $a = 2.36$ au, and each family had 1000 members. The vertical dashed lines mark the boundaries between the inner, middle and outer belts. The gap in the inner belt between $I \sim 15^\circ$ and 20° is related to the ν_6 secular resonance.

members are correlated to the initial inclination of the parent body. Therefore, the low-inclination population of non-vestoids indicated in Fig. 1 by red full circles could be pointing to a hypothetical parent body with initially low inclination.

We have also analysed the dependence on the mean ejection velocity and the initial number N of family members. In Fig. 4, we show the two extreme cases: a very compact family with 1000 members (in black) and a very extended family with 5000 members (in grey). The right-hand panel shows the final orbits of members scattered beyond 2.5 au. We have verified that the amount of the scattered orbits roughly scales linearly with N and that the larger initial dispersion of the family favours the scattering of orbits to longer distances. None of our simulations scatters orbits beyond 3.2 au (the 2J:-1A mean motion resonance is located at 3.2 au), in agreement with the fact that no confirmed V-type asteroid is currently known in that region of the belt.

In Table 1, we summarize the implantation probabilities obtained for each of the eight family configurations considered in our study. These probabilities represent the maximum values computed over the whole set of jumping Jupiter evolutions analysed here (which means that, for some evolutions, a given probability may actually be zero). We tested three target regions where orbits can be implanted. These correspond to the locations where the non-vestoids with no determined dynamical link to (4) Vesta or to the Vesta family are mostly found, i.e. the middle Main Belt, the outer Main Belt and the low-inclination inner Main Belt.

The implantation probabilities in the outer belt are an order of magnitude smaller than those in the middle belt. A family initially dispersed may implant up to two times more objects in the outer belt than an initially compact one. In the middle belt, however, the implanted probabilities show no significant dependence on the family compactness. A different situation is observed in the low-inclination inner belt, where the implantation probabilities are clearly correlated to the initial inclination of the family.

To determine how reliable are these probabilities, we estimate the number of asteroids, $N_{\rm src}$, that should be in the original hypothetical family to reproduce the currently observed populations in the three target regions. This is given by the formula

$$N_{\rm src} = \frac{N_{\rm obs}}{f_{\rm obs} \times p_{\rm imp} \times f_{\rm surv}}, \quad (1)$$

where $N_{\rm obs}$ is the number of V-type asteroids observed in the target region up to a given absolute magnitude H, $f_{\rm obs}$ is the fraction of all the existing V-type asteroids that have been observed up

Downloaded from https://academic.oup.com/mnras/article-abstract/468/1/1236/3059980 by Universidade Estadual Paulista Jï¿½lio de Mesquita Filho user on 19 June 2019

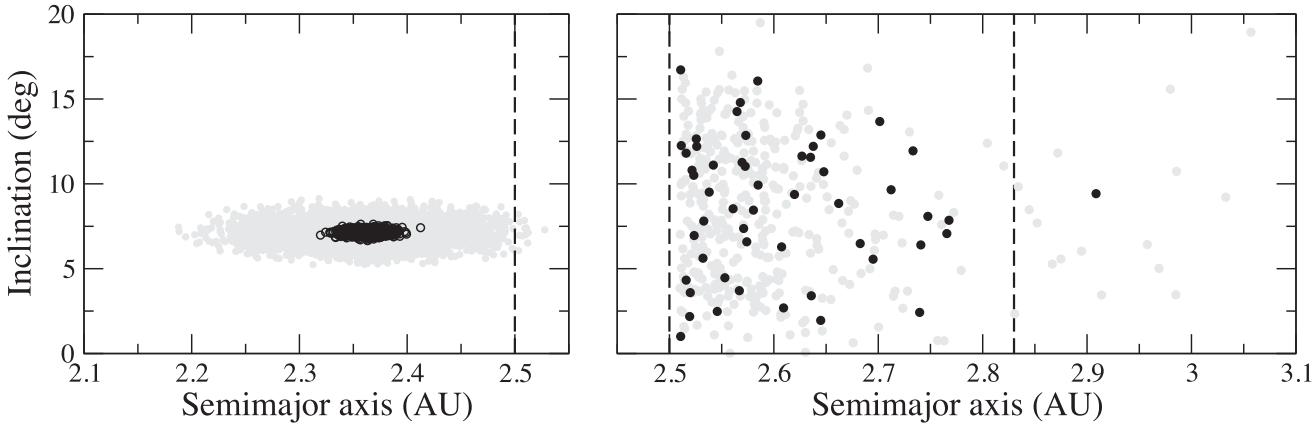

Figure 4. Left: the initial orbital distribution of two synthetic families in the inner belt generated using two different values of mean ejection velocity. The more compact family, shown in black, had 1000 members and corresponds to $\bar{v}_{ej} = 100$ m s^{-1} (same case as panel a of Fig. 3). The more extended family, shown in grey, had 5000 members and corresponds to $\bar{v}_{ej} = 400$ m s^{-1}. Right: final orbital distribution of the two families, for $a > 2.5$ au, after evolving through a jumping Jupiter instability (*case_1*).

Table 1. Maximum implantation probabilities in three different target regions obtained for the eight initial configurations considered in this study. Each configuration is identified with the same letter used in Fig. 3, and the asterisk (*) symbol refers to the much dispersed initial families with 5000 members. The target regions correspond to specific locations where non-vestoids are found (see the text).

Configuration	p_{imp}		
	Middle belt (%)	Outer belt (%)	Low-*I* inner belt (%)
(a)	10.0	0.8	40.9
(a)*	12.3	0.9	31.3
(b)	8.8	1.4	3.6
(b)*	10.1	0.9	3.7
(c)	11.0	0.6	21.8
(c)*	11.9	1.1	17.9
(d)	8.8	0.9	1.2
(d)*	9.9	1.5	1.3

to the same H, p_{imp} is the implantation probability in the target region given in Table 1 and f_{surv} is the fraction of implanted orbits after the instability that would be able to survive until present days.

In the spectroscopic sample, N_{obs} is well determined but it is not statistically significant, especially in the middle/outer belt. Moreover, the spectroscopic sample is strongly affected by observational biases related to the different surveys, which makes the determination of f_{obs} quite difficult. On the other hand, the SDSS or the MOVIS samples of V-type candidates provide more significant values of N_{obs} and allow for a more reliable determination of f_{obs}. To account for the fact that we are dealing with photometric candidates, we replace $N_{obs} = N_{cand} \times f_{conf}$, where N_{cand} is the actual number of candidates in the sample and f_{conf} is the fraction of these candidates that are expected to be confirmed as V-type by spectroscopic observations. Based on previous results by several authors (e.g. Jasmim et al. 2013, and references cited therein), we estimate that $f_{conf} \sim 0.8$.

To estimate f_{obs} for the SDSS or the MOVIS sample, we adopted two approaches. The first one consists in dividing the total number of Main Belt asteroids observed in either the SDSS or MOVIS sample by the total number of known Main Belt asteroids, considering a cut-off in absolute magnitude $H \leq 15$. According to Jedicke et al. (2015), this is the limiting magnitude for which the Main Belt sample is complete, and there are ~125 000 Main Belt asteroids with $H \leq 15$. From the SDSS and MOVIS samples, we get 20 600 (Carvano et al. 2010) and 17 200 (Popescu et al. 2016) Main Belt asteroids with $H \leq 15$, respectively. This gives a value of f_{obs} between 0.14 and 0.16. The second approach consists in dividing the number of SDSS or MOVIS V-type candidates found in the Vesta family by the total number of known members of the family, also with a cut-off $H \leq 15$. According to Nesvorný (2015b), there are 2408 members of the Vesta dynamical family with $H \leq 15$, but according to Licandro et al. (2017) only ~85 per cent of these would be actual V-type asteroids, which means ~2050 members. From the SDSS and MOVIS samples, we get 350 (Carvano et al. 2010) and 233 (Licandro et al. 2017) V-type candidates with $H \leq 15$, respectively. This implies a value of f_{obs} between 0.11 and 0.17, in good agreement with the previous estimate. Here, we will assume $f_{obs} = 0.15$.

Finally, to estimate f_{surv}, we use the simulations by Roig & Nesvorný (2015) and Nesvorný, Roig & Bottke (2017). These authors simulated the evolution of the primordial asteroid belt over the age of the Solar system considering four different phases: (i) the evolution before the jumping Jupiter instability during which the giant planets are in a compact orbital configuration and do no migrate, (ii) the evolution during the instability, (iii) the evolution after the instability during which the giant planets continue to migrate smoothly until the planetesimals disc is totally dispersed and the planets reach their present orbits (this phase of residual migration may last between 100 and 300 Myr) and (iv) the evolution after migration ceased until the present day (typically lasting ~4 Gyr). In the case of Nesvorný et al. (2017), the simulations include the gravitational perturbation of the terrestrial planets. This latter effect has proven to be relevant for the long-term depletion of the inner Main Belt after the jumping Jupiter instability, especially during phase (iv). Actually, the inner belt is depleted by a factor of ~2 compared to the simulations where the terrestrial planets are not considered. A similar behaviour is not observed in the middle and outer belts, where the long-term influence of the terrestrial planets is not so relevant. Based on these results, we estimate that, after the instability, the fractions of orbits that survive until today in the inner, the middle and the outer Main Belt are $f_{surv} = 0.14$, 0.66 and 0.59, respectively.

Downloaded from https://academic.oup.com/mnras/article-abstract/468/1/1236/3059980 by Universidade Estadual Paulista Jï¿½lio de Mesquita Filho user on 19 June 2019

Table 2. The estimated number $N_{\rm src}$ of asteroids with $H \leq 15$ that would be in the initial hypothetical family to reproduce the amount of observed SDSS or MOVIS non-vestoids $N_{\rm cand}$ in the different regions. For the low-inclination inner belt, we give two estimates depending on the two extreme values of $p_{\rm imp}$ obtained for the low/high initial inclination of the family. The last column gives the estimated diameter range of the crater that should be excavated to generate the hypothetical family, assuming a crater depth $h = 1$ km.

Region	$N_{\rm cand}$ (SDSS)	$N_{\rm cand}$ (MOVIS)	$N_{\rm src}$	$d_{\rm crat}$ (km)
Middle belt	23	13	850–2100	115–180
Outer belt	12	6	3600–18 000	240–540
			1500–12 700	160–450
Low-*I* inner belt	60	16	16 500–190 000	–

The resulting estimates of $N_{\rm src}$ for each target region are given in Table 2. These numbers can be compared to the ∼2400 members of the current Vesta family with $H \leq 15$ to conclude that a Vesta-like paleo-family could have been the source of many current non-vestoids in the three regions, scattered during the jumping Jupiter instability. The only clear exception is the case of a high-*I* paleo-family that produces totally unrealistic estimates for the low-*I* inner belt non-vestoids. This strengthens the conclusion that the very low inclination non-vestoids in the inner belt should be related to a parent body with a Vesta-like initial inclination. In the remaining cases, the upper limit estimates of $N_{\rm src}$ obtained for the three regions are not critical since the main source of uncertainty in the above calculations is the maximum $p_{\rm imp}$, which depends on the initial configuration of the family. These upper limit estimates may also be reduced by assuming that some of the non-vestoids in the three regions were not scattered by the jumping Jupiter instability, but have different origins.

Using the values of $N_{\rm src}$, we may estimate the total mass that should be excavated on the parent body. For this calculation, we assume that the cumulative size distribution of the fragments follows a power law $N(>D) = A\,D^{-\alpha}$ with exponent $\alpha = 5$. This is similar to the SFD of the current Vesta family in the range $2.1 \leq D \leq 8.0$ km (which corresponds to $12.1 \leq H \leq 15.0$ for albedo 0.4). The value of A is calibrated by imposing $N(>D_0) = N_{\rm src}$ for $D_0 = 2.1$ km ($H = 15$), and the diameter of the largest fragment is then given by $D_{\rm max} = A^{1/\alpha}$. The total mass excavated can be computed as

$$M(>D) = -\frac{\pi}{6}\rho\alpha A \int_{D_{\rm max}}^{D} D'^{-3(\alpha+1)}{\rm d}D', \tag{2}$$

where $\rho = 3.0$ g cm^{-3} is the typical density of basalt. Assuming that $N_{\rm src} \gg 1$ and $D_0 \geq D$, the above expression reduces to

$$M(>D) \simeq \frac{\pi}{6}\rho\frac{\alpha}{3\alpha+2}\frac{D_0^{\alpha}N_{\rm src}}{D^{3\alpha+2}}. \tag{3}$$

On the other hand, the excavated mass is roughly related to the size d and depth h of the corresponding crater (in km) through the formula

$$M \simeq \frac{\pi}{6}\rho h\left(\frac{3}{4}d^2 + h^2\right), \tag{4}$$

and equating (3) and (4) we obtain

$$d \simeq \left(\frac{4\alpha}{9\alpha+6}\frac{D_0^{\alpha}N_{\rm src}}{D^{3\alpha+2}h} - \frac{4}{3}h^2\right)^{1/2}. \tag{5}$$

The last column in Table 2 summarizes the estimated crater diameters assuming $D = 1$ km and a crater depth $h = 1$ km. If the depth is reduced to 0.5 km, the diameters increase by a factor of $\sqrt{2}$. Typical values of α may vary between 3 and 7, which implies that the diameters may be reduced/increased by a factor of up to 2. These diameters are smaller than or comparable to the diameters of the largest basins on the surface of Vesta.

We have also determined whether the final orbital distribution of implanted orbits reproduces the current distribution of the non-vestoids. Following Carruba et al. (2014) and Huaman et al. (2014), we have divided the middle and outer belts into seven subregions that according to these authors are dynamically isolated in the long term, i.e. asteroids have a low probability of migrating from one region to another even over Gyr time-scales. We have verified that our simulations are able to implant orbits in all the seven subregions depending on the initial configuration of the family and on the specific jumping Jupiter evolution. Table 3 shows the fractions of implanted orbits beyond 2.5 au that are implanted into each of the seven subregions. The fractions have been averaged over the different initial configurations of the family, separating the low-inclination configurations (e.g. panels a and c in Fig. 3) from the high-inclination ones (e.g. panels b and d in Fig. 3). The maximum and minimum values of each fraction reflect the effect of the different jumping Jupiter evolutions.

Several features can be addressed from these results. For example, the largest fraction of implanted bodies is concentrated in the interval 2.5–2.7 au. Some jumping Jupiter evolutions are not able to implant bodies beyond 2.7 au. Once again, there is a correlation between the initial inclination of the family and the final inclination of the implanted orbits, especially in the middle belt. The last row in Table 3 shows the fractions of the SDSS and MOVIS V-type candidates identified in the same seven subregions. In some regions, we observe a pretty good match, but in other regions the implanted fractions are either underestimated or overestimated by a factor that typically ranges between 2 and 5. In particular, our simulations do not seem to produce enough V-type asteroids in the outer Main Belt that is called the Eos region (sixth data column). We must bear in mind, however, that the fractions reported in the last two rows may be affected by poor statistics.

A final issue refers to the amount of fragments from the hypothetical family that would survive until present days in the inner belt (excluding the low-*I* region). These survivors are expected to be mixed today with the V-type asteroids created at later times by the Rheasilvia and Veneneia impact events. The amount of these bodies can be estimated as

$$N_{\rm src} \times (1 - f_{\rm deplet}) \times f_{\rm surv}, \tag{6}$$

where $f_{\rm deplet}$ is the fraction of orbits that are depleted from the inner belt during the jumping Jupiter instability, and $N_{\rm src}$ and $f_{\rm surv}$ are the parameters involved in equation (1). As previously shown, $N_{\rm src}$ ranges between 850 and 18 000, while $f_{\rm surv} = 0.14$ for the inner belt. The values of $f_{\rm deplet}$ can be determined from the simulations performed in this work, and we found values ranging between 0.4 and 0.9, mostly depending on the specific jumping Jupiter evolution. It is worth noting that the largest depletion fractions are provided precisely by the evolutions that are more efficient in implanting orbits into the middle/outer belt, so the large values of $f_{\rm deplet}$ should be preferred in equation (6) over the smallest ones. Therefore, using a compromise value of $f_{\rm deplet} = 0.7$, we obtain that the amount of surviving fragments would be something between 36 and 750 or even smaller. An additional depletion factor that may contribute to reduce even more of these numbers can be provided by the Yarkovsky effect, which is relevant for V-type asteroids with

Downloaded from https://academic.oup.com/mnras/article-abstract/468/1/1236/3059980 by Universidade Estadual Paulista Jï¿½lio de Mesquita Filho user on 19 June 2019

Table 3. Fractions of the implanted orbits that are implanted into each of the seven subregions defined in the middle and outer belts. Simulations are identified using the same convention as in Table 2. The last two rows provide the same fractions from the SDSS and MOVIS samples of V-type candidates.

Configurations	$2.5 \leq a < 2.71$ au		$2.71 \leq a < 2.83$ au		$2.83 \leq a < 2.97$ au	$2.97 \leq a < 3.28$ au	
	$I \leq 6.^{\circ}9$ (%)	$I > 6.^{\circ}9$ (%)	$I \leq 6.^{\circ}9$ (%)	$I > 6.^{\circ}9$ (%)	(%)	$I \leq 14.^{\circ}9$ (%)	$I > 14.^{\circ}9$ (%)
(a), (a)*, (c), (c)*	28.6–44.0	54.8–56.9	0–3.1	0–6.8	0–4.5	0.6–1.4	0–0.3
(b), (b)*, (d), (d)*	0–5.9	71.4–100	0–0.8	0–9.9	0–7.6	0–1.9	0–2.5
SDSS sample	32	26	8	14	6	13	1
MOVIS sample	16	37	5	11	0	26	5

$H \gtrsim 12$ over Gyr time-scales. Multiplying these number of survivors by the fraction of asteroids with known taxonomic classification, $f_{\rm obs} = 0.15$, we found that the number of currently observed V-type asteroids that may be related to a hypothetical Vesta-like paleo-family is between 5 and 110. This represents, for example, less than 13 per cent of the non-vestoid SDSS candidates in the inner belt (excluding the non-vestoids in the low-I region).

5 CONCLUSIONS

In this work, we have analysed the effect of the jumping Jupiter instability on a hypothetical primitive family of V-type asteroids in the inner belt. Our working hypothesis was that such family formed from a craterization event on the surface of (4) Vesta during the epoch of planetary migration of the giant planets, around or more than 4 Gyr ago. This hypothesis is supported by data from the Dawn mission and simulations of the collisional history of (4) Vesta (Pirani & Turrini 2016). Our main conclusions can be summarized as follows.

(i) The jumping Jupiter instability is able to scatter some of the V-type asteroids of this hypothetical family into regions of the Main Belt that otherwise could not be reached by long-term dynamical evolution. This mechanism may explain, at least partially, the population of non-vestoids observed in the middle and outer belts.

(ii) The instability can also explain the population of non-vestoids with very low inclinations in the inner belt ($I \lesssim 5^{\circ}$), provided that the parent body had a Vesta-like inclination ($\sim 7^{\circ}$).

(iii) We estimate that the diameter of the crater that has to be excavated to originate the hypothetical primitive family ranges between 100 and 500 km. According to Pirani & Turrini (2016), traces of such a basin might have been erased by the subsequent collisional history of (4) Vesta.

(iv) We estimate that $\sim$10 per cent or less of the currently observed V-type asteroids in the inner belt may be relics of this primitive family.

(v) Although the jumping Jupiter instability can implant inner belt asteroids in Magnya-like orbits, this is not enough to explain the origin of (1459) Magnya. The typical implantation probabilities imply that in order to obtain (1459) Magnya there should have been several tens of V-type asteroids with $D \sim 20$ km in the original source. This hypothesis is incompatible with a craterization event and is not supported by observations since no other V-type asteroid in this size range has been detected so far.

(vi) Our model suggests that many non-vestoids, including those in the middle/outer belt – except (1459) Magnya, should be genetically related to (4) Vesta but not to the current Vesta family. Observational evidence from spectroscopy and polarimetry, in principle, is not incompatible with this idea.

(vii) (1459) Magnya continues to be a unique piece of basaltic material whose origin is still an open question.

ACKNOWLEDGEMENTS

We wish to thank the helpful comments and criticism of the referees. PIOB and FR acknowledge support from the Brazilian Council of Research (CNPq). DN is supported by NASA's Emerging Worlds program and Brazil's Science without Borders program. VC is supported by the São Paulo State Science Foundation (FAPESP).

REFERENCES

Binzel R. P., Xu S., 1993, Science, 260, 186
Bottke W. F. Jr., Vokrouhlický D., Rubincam D. P., Broz M., 2002, in Bottke W. F. Jr., Cellino A., Paolicchi P., Binzel R. P., eds, Asteroids III. Univ. Arizona Press, Tucson, AZ, p. 395
Brasil P. I. O., Nesvorný D., Gomes R. S., 2014, AJ, 148, 56
Brasil P. I. O., Roig F., Nesvorný D., Carruba V., Aljbaae S., Huaman M. E., 2016, Icarus, 266, 142
Brasser R., Morbidelli A., Gomes R., Tsiganis K., Levison H. F., 2009, A&A, 507, 1053
Buratti B. J. et al., 2013, J. Geophys. Res.: Planets, 118, 1991
Burbine T. H., Buchanan P. C., Binzel R. P., Bus S. J., Hiroi T., Hinrichs J. L., Meibom A., McCoy T. J., 2001, Meteoritics Planet. Sci., 36, 761
Bus S. J., Binzel R. P., 2002, Icarus, 158, 146
Carruba V., Michtchenko T. A., Roig F., Ferraz-Mello S., Nesvorný D., 2005, A&A, 441, 819
Carruba V., Roig F., Michtchenko T. A., Ferraz-Mello S., Nesvorný D., 2007a, A&A, 465, 315
Carruba V., Michtchenko T. A., Lazzaro D., 2007b, A&A, 473, 967
Carruba V., Huaman M. E., Domingos R. C., Santos C. R. D., Souami D., 2014, MNRAS, 439, 3168
Carruba V., Nesvorný D., Aljbaae S., Domingos R. C., Huaman M., 2016, MNRAS, 458, 3731
Carvano J. M., Hasselmann P. H., Lazzaro D., Mothé-Diniz T., 2010, A&A, 510, A43
Cellino A. et al., 2016, MNRAS, 456, 248
Deienno R., Nesvorný D., Vokrouhlický D., Yokoyama T., 2014, AJ, 148, 25
Delbo M. et al., 2006, Icarus, 181, 618
DeMeo F. E., Binzel R. P., Slivan S. M., Bus S. J., 2009, Icarus, 202, 160
de Sanctis M. C., Ammannito E., Migliorini A., Jasmim F. L., Lazzaro D., Marchi S., Filacchione G., Capria M. T., 2011a, EPSC-DPS Joint Meeting 2011. p. 215 (http://meetings.copernicus.org/epsc-dps2011)
de Sanctis M. C., Migliorini A., Luzia Jasmin F., Lazzaro D., Filacchione G., Marchi S., Ammannito E., Capria M. T., 2011b, A&A, 533, A77
Duffard R., Roig F., 2009, Planet. Space Sci., 57, 229
Duffard R., Lazzaro D., Licandro J., De Sanctis M. C., Capria M. T., 2006, Adv. Space Res., 38, 1987
Durda D. D., Bottke W. F., Nesvorný D., Enke B. L., Merline W. J., Asphaug E., Richardson D. C., 2007, Icarus, 186, 498
Fernandez J. A., Ip W.-H., 1984, Icarus, 58, 109
Folonier H. A., Roig F., Beaugé C., 2014, Celest. Mech. Dyn. Astron., 119, 1
Gil-Hutton R., López-Sisterna C., Calandra M. F., 2017, A&A, 599, 114
Grimm R. E., McSween H. Y., 1993, Science, 259, 653
Hardersen P. S., Gaffey M. J., Abell P. A., 2004, Icarus, 167, 170

Downloaded from https://academic.oup.com/mnras/article-abstract/468/1/1236/3059980 by Universidade Estadual Paulista Jï¿½lio de Mesquita Filho user on 19 June 2019

Huaman M. E., Carruba V., Domingos R. C., 2014, MNRAS, 444, 2985
Ieva S., Dotto E., Lazzaro D., Perna D., Fulvio D., Fulchignoni M., 2016, MNRAS, 455, 2871
Jasmim F. L., Lazzaro D., Carvano J. M. F., Mothé-Diniz T., Hasselmann P. H., 2013, A&A, 552, A85
Jedicke R., Granvik M., Micheli M., Ryan E., Spahr T., Yeomans D. K., 2015, in Michel P., DeMeo F. E., Bottke W. F., eds, Asteroids IV. Univ. Arizona Press, Tucson, AZ, p. 795
Lazzaro D. et al., 2000, Science, 288, 2033
Licandro J., Popescu M., de Leon J., Morate D., 2017, A&A, in press
McCord T. B., Adams J. B., Johnson T. V., 1970, Science, 168, 1445
McSween H. Y. et al., 2013, J. Geophys. Res.: Planets, 118, 335
Marchi S. et al., 2012, Science, 336, 690
Michel P., Richardson D. C., Durda D. D., Jutzi M., Asphaug E., 2015, in Michel P., DeMeo F. E., Bottke W. F., eds, Asteroids IV. Univ. Arizona Press, Tucson, AZ, p. 341
Michtchenko T. A., Lazzaro D., Ferraz-Mello S., Roig F., 2002, Icarus, 158, 343
Michtchenko T. A., Lazzaro D., Carvano J. M., 2016, A&A, 588, A11
Migliorini A., De Sanctis M. C., Lazzaro D., Ammannito E., 2017, MNRAS, 464, 1718
Milani A., Cellino A., Knežević Z., Novaković B., Spoto F., Paolicchi P., 2014, Icarus, 239, 46
Morbidelli A., Brasser R., Tsiganis K., Gomes R., Levison H. F., 2009, A&A, 507, 1041
Moskovitz N. A., Jedicke R., Gaidos E., Willman M., Nesvorný D., Fevig R., Ivezić Ž., 2008, Icarus, 198, 77
Nathues A., Mottola S., Kaasalainen M., Neukum G., 2005, Icarus, 175, 452
Nesvorný D., 2011, ApJ, 742, L22
Nesvorný D., 2015a, AJ, 150, 68
Nesvorný D., 2015b, NASA Planetary Data System, EAR-A-VARGBDET-5-NESVORNYFAM-V3.0
Nesvorný D., Morbidelli A., 2012, AJ, 144, 117
Nesvorný D., Roig F., Gladman B., Lazzaro D., Carruba V., Mothé-Diniz T., 2008, Icarus, 193, 85
Nesvorný D., Vokrouhlický D., Morbidelli A., 2013, ApJ, 768, 45
Nesvorný D., Vokrouhlický D., Deienno R., Walsh K. J., 2014a, AJ, 148, 52
Nesvorný D., Vokrouhlický D., Deienno R., 2014b, ApJ, 784, 22
Nesvorný D., Roig F., Bottke W. F. Jr., 2017, AJ, 153, 103
O'Brien D. P., Marchi S., Morbidelli A., Bottke W. F., Schenk P. M., Russell C. T., Raymond C. A., 2014, Planet. Space Sci., 103, 131
Pirani S., Turrini D., 2016, Icarus, 271, 170
Popescu M. et al., 2016, A&A, 591, A115
Ribeiro A. O., Roig F., 2011, J. Phys. Conf. Ser., 285, 012024
Roig F., Gil-Hutton R., 2006, Icarus, 183, 411
Roig F., Nesvorný D., 2015, AJ, 150, 186
Roig F., Nesvorný D., Gil-Hutton R., Lazzaro D., 2008, Icarus, 194, 125
Russell C. T. et al., 2012, Science, 336, 684
Schenk P. et al., 2012, Science, 336, 694
Tsiganis K., Gomes R., Morbidelli A., Levison H. F., 2005, Nature, 435, 459
Zuber M. T., McSween H. Y., Binzel R. P., Elkins-Tanton L. T., Konopliv A. S., Pieters C. M., Smith D. E., 2011, Space Sci. Rev., 163, 77

This paper has been typeset from a TEX/LATEX file prepared by the author.

Downloaded from https://academic.oup.com/mnras/article-abstract/468/1/1236/3059980 by Universidade Estadual Paulista Jï¿½lio de Mesquita Filho user on 19 June 2019